Journal of Medicinal Chemistry

Article

pubs.acs.org/jmc

Synthesis and Biological Characterization of Protease-Activated Prodrugs of Doxazolidine

Benjamin L. Barthel, Daniel L. Rudnicki, Thomas Price Kirby, Sean M. Colvin, David J. Burkhart,[†] and Tad H. Koch*

Department of Chemistry and Biochemistry, University of Colorado, Boulder, Colorado 80309-0215, United States

Supporting Information

ABSTRACT: Doxazolidine (doxaz) is a new anthracycline anticancer agent. While structurally similar to doxorubicin (dox), doxaz acts via a distinct mechanism to selectively enhance anticancer activity over cardiotoxicity, the most significant clinical impediment to successful anthracycline treatment. Here, we describe the synthesis and characterization of a prodrug platform designed for doxaz release mediated by secreted proteolytic activity, a common association with invasiveness and poor prognosis in cancer patients. GaFK-Doxaz is hydrolyzable by the proteases plasmin and cathepsin B, both strongly linked with cancer progression, as well as trypsin. We demonstrate that activation of GaFK-Doxaz releases highly potent doxaz that powerfully inhibits the growth of a wide variety of cancer cells (average IC_{50} of 8 nM). GaFK-Doxaz is stable in human plasma and is poorly membrane permeable, thereby limiting activation to locally secreted proteolytic activity and reducing the likelihood of severe side effects.

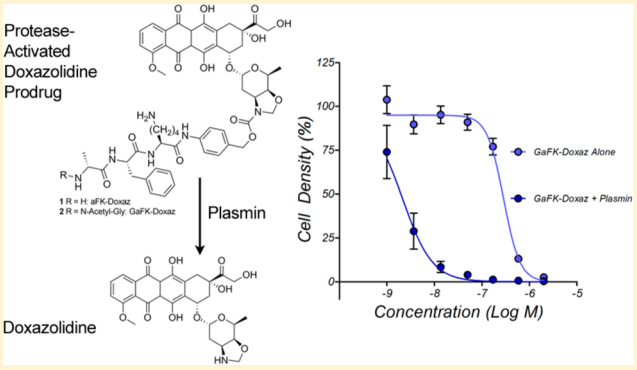

INTRODUCTION

Doxorubicin (dox) is a successful and widely used anthracycline anticancer agent and is a common component in many protocols for treatment of both solid and nonsolid tumors. Its efficacy is tempered by a considerable dose-dependent cardiotoxic side effect, potentially leading to drug-refractory congestive heart failure years after the cessation of treatment.[1,2] Additionally, tumors can gain resistance to dox therapy, primarily via the multidrug-resistance phenotype (MDR) and elevated expression of P170 glycoprotein (P170GP).[3] Consequently, the clinical attitude toward dox is one of ambivalence. Although a large body of evidence suggests that the cardiotoxicity and antitumor activity are derived from distinct mechanisms (oxidative damage and topoisomerase II inhibition, respectively),[2,4,5] extensive research into compounds and formulations that selectively enhance the anticancer activity has produced few clinically relevant variants. Commonly, patients are treated with an additional, iron-sequestering compound, dexrazoxane (ICRF-187), to dampen the iron-dependent redox chemistry that leads to the liberation of reactive oxygen species and damage to cardiac tissue.[6] Formulations in which the drug is encapsulated in a naked liposome or a polyethylene glycol (PEG) coated liposome have successfully improved the therapeutic index but, particularly for PEG-coated formulations, introduce a dose-limiting hand–foot syndrome side effect.[7−9]

In 2005, we described a variant of dox that demonstrated a selective enhancement of antitumor activity.[10] Termed doxazolidine (doxaz), the new compound is a conjugate of dox with 1 equiv of formaldehyde, which links the 3′-amino and 4′-hydroxyl groups to form an oxazolidine ring (Scheme 1). Doxaz is much more toxic to cancer cells compared to dox, with IC_{50} values between 1 and 4 orders of magnitude lower, and its potency is not affected by P170GP expression. The increased cytotoxic activity of doxaz is tumor selective because doxaz and dox are equally toxic against a rat cardiomyocyte cell line. These observations and additional investigations indicated that doxaz is mechanistically distinct from dox and is not dependent upon topoisomerase II.[11] Instead, doxaz is a DNA alkylating agent at sites of 5′-GC-3′, where it forms a covalent bond via the formaldehyde carbon to one guanine and hydrogen-bonds to the guanine on the opposite strand.[10,12]

The distinct advantages that doxaz has over dox make it an attractive potential clinical agent. However, doxaz is very short-lived; under physiological conditions, hydrolysis and loss of the formaldehyde result in its conversion to dox with a half-life of approximately 3 min.[10] Therefore, we undertook the development of various prodrug strategies, in which doxaz is inactivated and stabilized until being selectively released by environmental conditions present in the microenvironment of the tumor. A first-generation doxaz prodrug, pentyl PABC-Doxaz (PPD), was designed for activation by human carboxylesterase 2 (CES2, hiCE) and demonstrated an in vivo antitumor efficacy against CES2-positive xenografts that was better than or equal to that of

Received: May 21, 2012
Published: June 28, 2012

Scheme 1. Synthesis of doxaz and Structure of Protease-Activated doxaz Prodrugs[a]

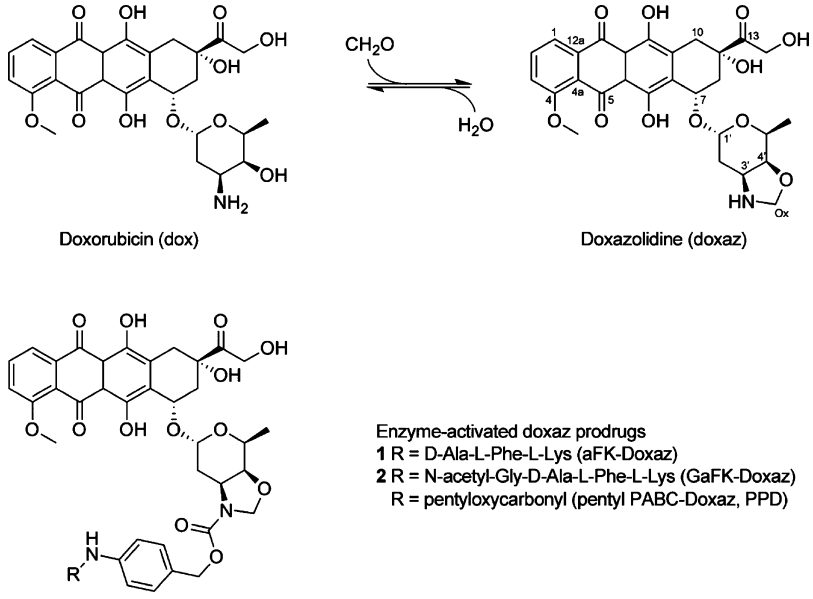

[a]Doxorubicin was converted to doxazolidine by reaction with a molecule of formaldehyde at the exocyclic amine and alcohol groups of the daunosamine sugar and loss of water. This results in an oxazolidine ring, which can be readily hydrolyzed, losing the formaldehyde, back to dox with a physiological half-life of approximately 3 min at 37 °C and pH 7.[10] Enzyme-activated prodrugs of doxaz, which are stabilized by acylation of the oxazolidine nitrogen, incorporate an enzyme-cleavable trigger (R) separated from the drug by a spacer derived from p-aminobenzyl alcohol. Protease-activated doxaz prodrug containing the triggers D-ala-L-Phe-L-Lys (aFK-Doxaz, **1**) and N-acetyl-Gly-D-ala-L-Phe-L-Lys (GaFK-Doxaz, **2**) are described here, while the carboxylesterase-activated doxaz prodrug PPD, where the trigger is pentyloxycarbonyl, has been described previously.[13]

Scheme 2. Protease Activation of doxaz Prodrugs[a]

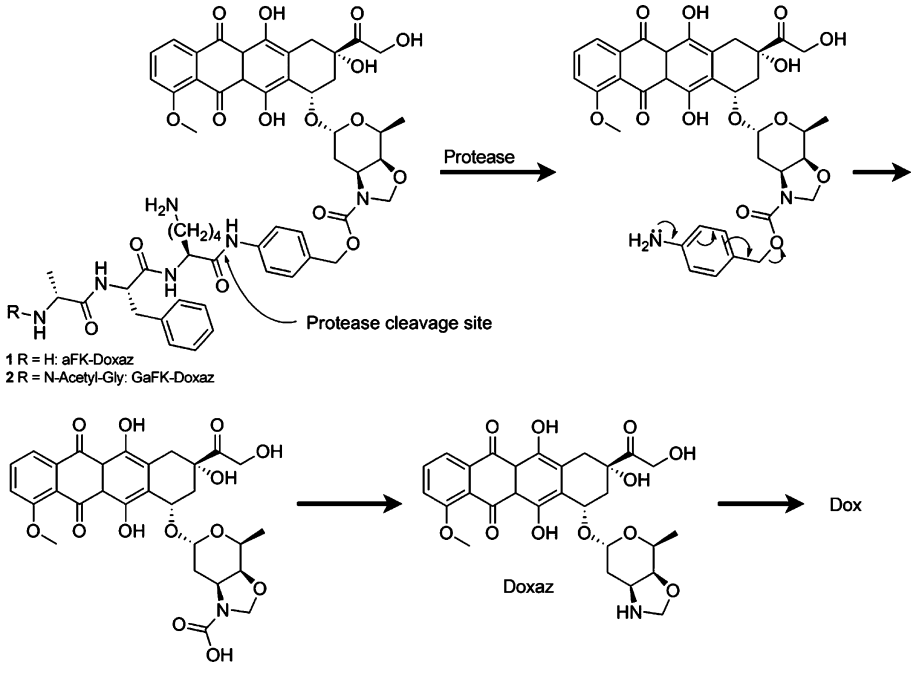

[a]Activation occurs through protease-mediated hydrolysis of the Lys-PABC amide bond. The resulting unstable intermediate undergoes a spontaneous 1,6 elimination, releasing an iminoquinone methide and the unstable carbamic acid of doxaz. Spontaneous decarboxylation liberates free doxaz, which readily cross-links DNA or hydrolyzes to dox under physiological conditions.

dox.[13−15] Moreover, PPD was effective without producing the severe cardiac damage characteristic of dox. However, despite being important for activation of the clinical anticancer agents irinotecan and capecitabine, CES2 is not a reliable marker for tumor tissue.[16] PPD, therefore, is limited in its scope and not a candidate for wide-spectrum therapy but is a proof of concept for anticancer agents based upon prodrug delivery of doxaz.

Proteolytic activity, on the other hand, is a very common and widespread indicator of neoplastic tissues. In addition to creating the physical space required for invasion and metastasis, tumor-

dx.doi.org/10.1021/jm300714p | J. Med. Chem. 2012, 55, 6595−6607

Scheme 3. Synthesis of Protease-Activated Prodrug Triggers[a]

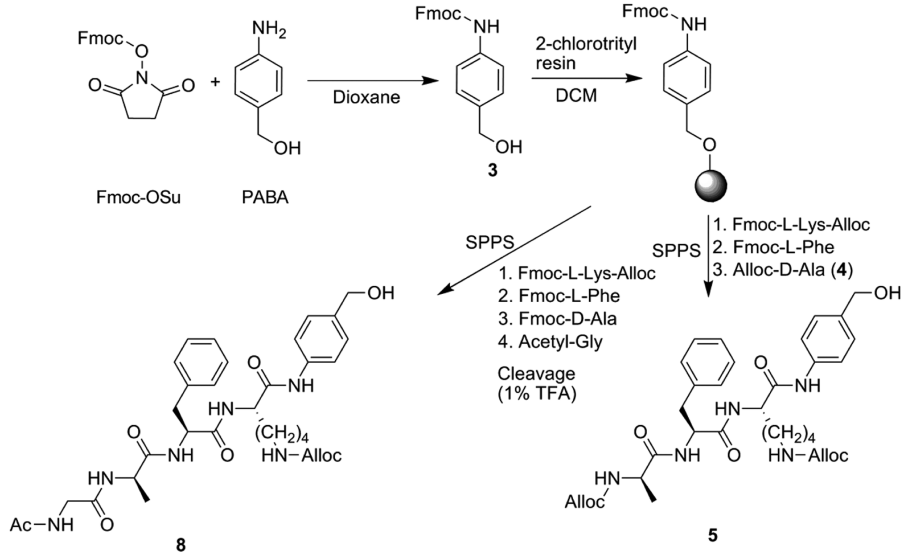

[a]Fmoc-protected PABA (**3**) was synthesized from commercially available starting materials and loaded onto 2-chlorotrityl resin. Solid-phase peptide synthesis (SPPS) of bis-alloc-aFK-PABA (**5**) and *N*-acetyl-GaFK(alloc)-PABA (**8**) was achieved with Fmoc-protected amino acids followed by cleavage from resin with TFA. Alloc-D-Ala (**4**) used in synthesis of **5** is described in Supporting Information.

Scheme 4. Coupling of Peptide Trigger to Doxazolidine[a]

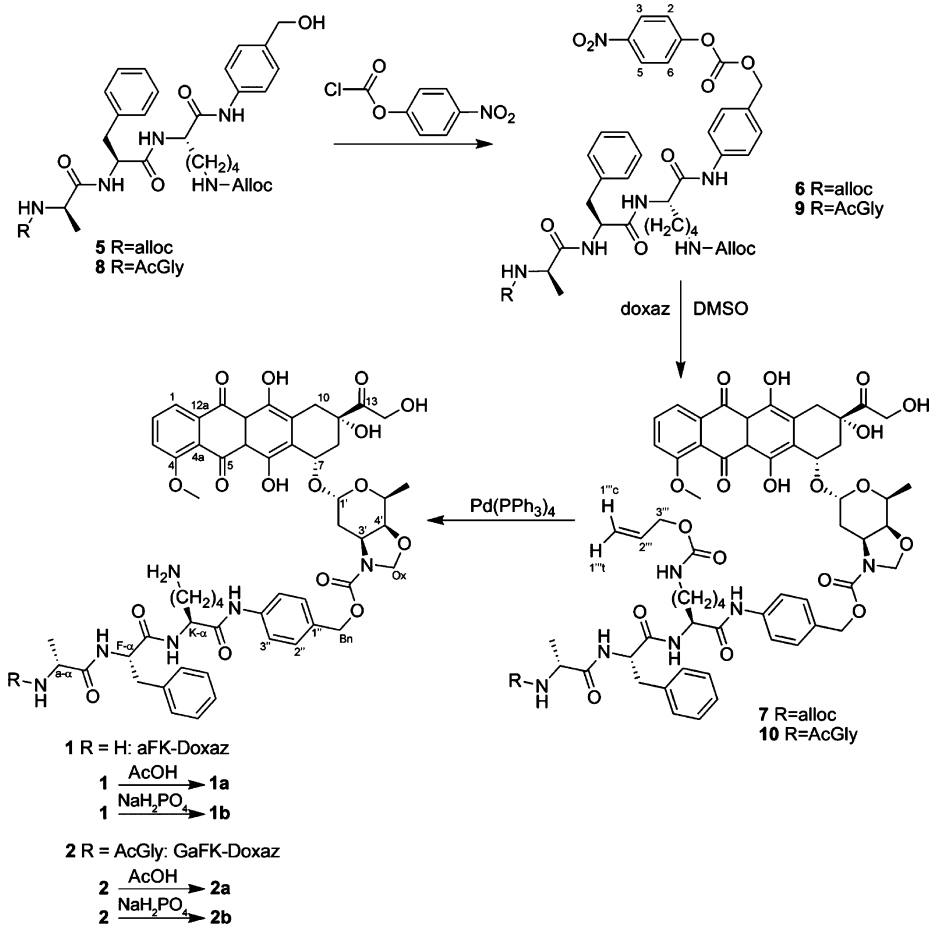

[a]Activation of **5** or **8** to the mixed carbonates **6** and **9** was followed by reaction with doxaz to produce the protected prodrugs **7** and **10**. Deprotection of the alloc groups was accomplished with tetrakis(triphenylphosphine)palladium(0) to liberate the free bases **1** and **2**. Acidification resulted in either the acetate or phosphate salts of **1** (**1a** or **1b**, respectively) and **2** (**2a** or **2b**, respectively).

dx.doi.org/10.1021/jm300714p | *J. Med. Chem.* 2012, 55, 6595−6607

expressed proteases can take on a more active role in the tumorigenic transformation and development, primarily through the liberation and activation of extracellular matrix (ECM) associated growth factors and cytokines.[17−20] Of particular interest is the plasmin system, in which the zymogen plasminogen is converted to active plasmin at or near the cell surface by surface-bound urokinase-type plasminogen activator (uPA). Plasmin can then degrade the ECM and basement membrane components directly or indirectly through activation of a variety of other proteolytic proenzymes, including the matrix metalloproteases (MMPs).[21] Not surprisingly, high levels of plasmin pathway components often correlate with poor prognosis in a wide panel of tumor types (see review by Ulisse[22]), including difficult to treat cancers such as lung,[23−25] liver,[26,27] and pancreas.[28−30]

Given the widespread significance of proteolytic activity in tumor progression, metastasis, and overall prognosis, coupled with its relative absence for normal, static tissues, proteolytic activity makes an attractive tumor-selective filter and tool for prodrug activation. Many protease-activated prodrug strategies have been designed and characterized for many different cytotoxic chemotherapeutics, including dox. In 1999, de Groot and colleagues described a prodrug for dox in which activation was accomplished by plasmin cleavage of a tripeptide, followed by self-elimination of a spacer unit.[31] In animal models, this prodrug exhibited antitumor efficacy with a significantly better toxicity profile than dox.[32] Here, using this design as a model, we describe the synthesis and characterization of a similar prodrug for protease-activated delivery of doxaz, a significantly more active anthracycline.

RESULTS AND DISCUSSION

Strategy, Design, and Synthesis of aFK-Doxaz (1). Our initial design and proposed synthesis of **1** paralleled that of the plasmin-activated prodrug of dox published by de Groot et al.[31] Enzyme recognition is afforded by the tripartate amino acid enzyme recognition sequence D-alanine-L-phenylalanine-L-lysine (aFK) coupled via an arylamide bond to the *p*-aminobenzyl alcohol (PABA) derived Katzenellenbogen spacer,[33] which is coupled to the daunosamine sugar moiety of the anthracycline to form the carbamate prodrug. Upon enzymatic cleavage at the carboxyl end of the lysine, the liberated aniline undergoes a spontaneous 1,6 elimination to release the iminoquinone methide and, following decarboxylation of the carbamic acid, release of the active therapeutic (Scheme 2).

In de Groot's synthesis, the tripeptide was prepared using solution-phase chemistry and subsequently coupled to PABA. Our synthetic strategy differed only in that we used solid-phase peptide synthesis (SPPS) and built the peptide directly onto resin-bound PABA (Scheme 3). Fmoc-PABA (**3**) was formed in high yield by reaction of Fmoc-OSu with commercially available PABA in dry dioxane and was subsequently etherified by loading onto a 2-chlorotrityl chloride polystyrene resin. SPPS proceeded by standard Fmoc chemistry using Fmoc-L-Lys(N_ε-alloc), Fmoc-L-Phe, and alloc-D-Ala (**4**), which was prepared from commercially available D-Ala and allyl chloroformate. Coupling of Fmoc-L-Lys to PABA was allowed to proceed for 16 h owing to the poor nucleophilicity of the aniline, but standard 1 h coupling times afforded high yields of the remaining carboxamide couplings. Following cleavage from the resin with trifluoroacetic acid to yield the free protected peptido-PABA (**5**) and subsequent activation to the *p*-nitrophenyl carbonate of alloc-aFK(alloc)-PABA (**6**), the bis-alloc protected carbamate prodrug **7** was formed by coupling to doxaz (Scheme 4). This was a slow and poor-yielding reaction, typically requiring approximately 7−10 days to reach 85−90% completion by RP-HPLC and resulted in only a 33% isolated yield following radial silica gel chromatography. This reaction also yielded a small amount of alloc-aFK(alloc)-PABC-Dox due to hydrolysis of the doxaz by adventitious water and more rapid reaction of dox than doxaz. For use as a control in future efficacy comparisons, this material was also purified and deprotected.

Final deprotection of the alloc groups by palladium-catalyzed allyl transfer to morpholine was accomplished with tetrakis-(triphenylphosphine) Pd^0 with subsequent acidification (Scheme 4). Initially, this acidification was performed with acetic acid to yield the bis-acetate salt of aFK-Doxaz (**1a**). However, ^{1}H NMR analysis of the crude reaction mixture indicated the presence of a side product representing approximately 15% of the total anthracycline composition. This impurity was tentatively assigned to be the diastereomer of aFK-Doxaz arising from epimerization of the α-methyl group of the N-terminal alanine residue based on chemical shift analysis. All other peaks appeared as expected, and integration of the duplicated alanine α-methyl signals summed to equal the integration of the 5′-methyl peak on the daunosamine sugar was consistent with the anticipated 1:1 molar ratio of the respective moieties. A homonuclear gradient COSY experiment also confirmed coupling between the suspected L-alanine α-methyl and α-proton signals, consistent with our assignment of the impurity as the diastereomer resulting from Ala epimerization. RP-HPLC was able to distinguish the two diastereomers, but poor chromatographic resolution prevented isolation of sufficient quantities of spectroscopically pure materials. Modification of the proposed synthesis was therefore required to reduce the abundance of the diastereomer in order to simplify biological characterization.

We hypothesized that the epimerization was occurring as a result of the acidification procedure following the final alloc-deprotection reaction. Additional attempts to salt-out the product by varying the temperature, time, and acidic reagent failed to yield satisfactory results. Moreover, no gains in purity were made during our exploration of various amino-protecting groups, including ^{t}Boc, Fmoc, and TFA. Nevertheless, while additional synthetic routes were being explored, we successfully isolated small quantities of prodrug by RP-HPLC purification to yield the pure bis-phosphate salt of aFK-Doxaz (**1b**) and the bis-acetate salt of aFK-Dox.

Biological Characterization of the Bis-phosphate Salt of aFK-Doxaz (1b). Given that the challenges of the synthesis of plasmin-activated doxaz prodrugs limit the efficiency and scalability of the synthesis of aFK-Doxaz (**1b**), a limited biological characterization of **1b** was undertaken while new synthetic routes were being explored. This characterization focused on demonstrating that **1b** could be hydrolyzed by plasmin and proving that plasmin hydrolysis released doxaz and not dox.

To test the ability of plasmin to cleave **1b**, we incubated 50 μM **1b** with 3.3 μg/mL plasmin in PBS at 37 °C. The reaction progress was monitored by RP-HPLC; small samples were removed from the reaction at various times and analyzed for the presence of the anthracycline chromophore by absorbance at 480 nm. Because of the instability of doxaz under aqueous conditions, doxaz is rarely, if ever, directly observed by RP-HPLC. Instead, its formation was inferred by the presence of dox over the time course. As expected, plasmin readily catalyzed the hydrolysis of

1b (Figure 1), and in the absence of enzyme, **1b** was fully stable (data not shown).

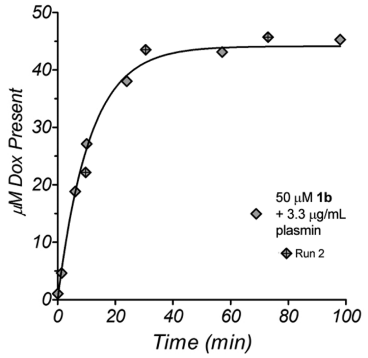

Figure 1. RP-HPLC analysis of an enzymatic reaction between 50 μM **1b** and 3.3 μg/mL human plasmin. The reaction was performed at pH 7.4 in PBS at 37 °C. A second measurement using slightly different reaction times is shown as diamonds with crosses (run 2). The data were fit using nonlinear least-squares analysis with a single-exponential association model.

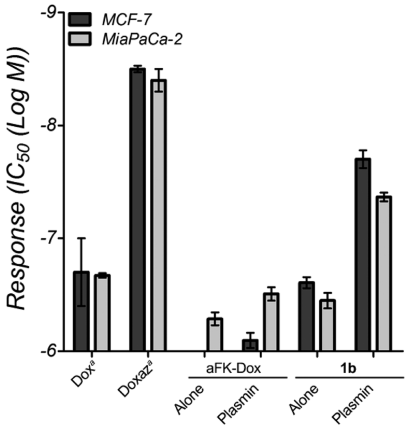

Figure 2. Response of MCF-7 breast cancer cells (dark bars) and MiaPaCa-2 pancreatic cancer cells (light bars) to dox, doxaz, aFK-Dox, and **1b**. The two prodrugs were tested in the absence or presence of plasmin. Response is measured by the IC_{50} in units of log *M*, and the values are the average of at least six measurements. The toxicity of aFK-Dox toward MCF-7 cells was outside the concentration range of the experiment (>−6). The error bars represent the standard error. [a]IC_{50} values for dox and doxaz are from ref 13.

The cell-free HPLC analysis of enzymatic hydrolysis, coupled with the ^{1}H NMR verification that doxaz was intact in the final prodrug, suggests that plasmin was catalyzing the release of doxaz, which then quickly hydrolyzed to dox before the analysis of the reaction. In theory, the presence of a serine protease likely has little to no effect on the half-life of the liberated doxaz. However, because of the inability of HPLC to differentiate between release of dox and release of doxaz, we do not know from the above experiment whether activation of **1b** released doxaz or dox. Since doxaz is so much more cytotoxic than dox despite its short lifetime, a cell-based comparison of **1b** and aFK-Dox can distinguish a prodrug that releases doxaz from one that releases dox. Two cell lines were chosen for this analysis: the human breast carcinoma line MCF-7 and the human pancreatic carcinoma line MiaPaCa-2. In a 3 h treatment, followed by 3−4 days of growth (until DMSO-only treatment lanes reached 80% confluency), the dox and doxaz prodrugs produced dramatically different growth inhibition profiles and IC_{50} values (Figure 2). In both cell lines, **1b** was more toxic than aFK-Dox when treated with drug alone. This activity likely reflects the endogenous activation of cell-expressed plasminogen to plasmin. Additionally, **1b** alone was equally or more toxic in both lines than the combination of aFK-Dox and plasmin, and adding plasmin to **1b** increased this difference substantially, exhibiting greater toxicity than treating with fully active dox alone. Taken together, these data confirm that **1b** releases doxaz, rather than dox, in a plasmin-dependent manner. Further, considering the previously reported preclinical advantages conferred by aFK-Dox,[32] these results suggest that further development of protease-activated doxaz prodrugs may produce a potent, clinically attractive targeted anticancer drug.

Strategy, Design, and Synthesis of GaFK-Doxaz (2). Preliminary characterizations of **1b** demonstrated that plasmin-activated doxaz prodrugs have potential as effective anticancer compounds and are significantly more efficacious than similar dox prodrugs. However, formation of the alanine epimer prevented isolation of sufficient quantities of pure material for wider biological analyses. Modification of the deprotection conditions proved unsatisfactory, but we hypothesized that the epimerization might be circumvented altogether with the addition of the commercially available protected amino acid, *N*-acetyl glycine, at the N-terminus of the peptide. Glycine incorporation would negate the N-terminal amino acid's α-proton acidity by placing an achiral residue at this position and eliminate the need for removal of two alloc groups in the final deprotection step. Additionally, the presence of *N*-acetyl protection of the amino terminus may provide resistance against exopeptidase activity.[34−36] Small-scale synthesis of GaFK-Doxaz (**2**) yielded a single diastereomer (>95% purity by RP-HPLC) without significant reduction of the yield as a result of the additional deprotection, activation, and coupling reactions. We therefore undertook a scaled synthesis of **2** and present a more comprehensive biological characterization.

Analogous to the synthesis of **1b**, *N*-Ac-GaFK(alloc)-PABA (**8**) was prepared by SPPS (Scheme 3) and subsequently transformed to the mixed carbonate (**9**, Scheme 4). Coupling of **9** with doxaz to form the protected peptidyl prodrug (**10**) was improved by addition of 1-hydroxybenzotriazole (HOBt) to the reaction mixture, resulting in complete consumption of the starting anthracycline after 72 h, as measured by RP-HPLC. Preparative HPLC purification gave **10** in 46% yield. Deprotection of the lysine ε-amino group with tetrakis-(triphenylphosphine)palladium(0) was carried out in dichloromethane acidified with acetic acid to yield the acetate salt of AcGaFK-PABC-Doxaz (**2a**). ^{1}H NMR of the crude salt revealed a significant amount of contaminating triphenylphosphine oxide, due to oxidation of the deprotection catalyst. This contaminant, in early preparations, persisted through the final RP-HPLC purification and was removed from subsequent preparations by washing an aqueous solution of **2a** with ethyl acetate. The crude product was purified by preparative RP-HPLC from a C-18 column and isocratic conditions of 1:1 acetonitrile/20 mM phosphate buffer, pH 4.6−4.8, to give the pure phosphate salt (**2b**), which was formulated in PEG-400 in saline (10% v/v) with a yield of 78%.

Enzyme Kinetics of Activation. The rate and kinetics of hydrolysis of **2b** were measured by RP-HPLC, monitoring the dox released from doxaz hydrolysis after enzyme-mediated cleavage of **2b**. In a time course of activation, 50 μM **2b** was

dx.doi.org/10.1021/jm300714p | J. Med. Chem. 2012, 55, 6595−6607

incubated at 37 °C with 1.2 μg/mL human plasmin in PBS. As expected from our characterization of **1b**, dox was quickly produced and the prodrug nearly fully consumed by 2 h, indicating release of doxaz, which then quickly degraded to dox (Figure 3). In separate reactions containing no enzyme, there

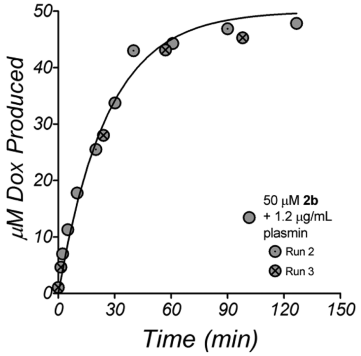

Figure 3. RP-HPLC analysis of an enzymatic reaction between 50 μM **2b** and 1.2 μg/mL human plasmin. The reaction was performed in PBS, pH 7.4, at 37 °C. Repeated measurements with slightly different reaction times are shown as either circles with included dots (run 2) or crosses (run 3). The combined data were fit using nonlinear least-squares analysis with a single-exponential association model.

was no observable increase in dox over the course of 24 h, showing that **2b** is stable in the absence of enzyme. To simplify downstream analyses, we made measurements of the activity of plasmin using **2b** as a substrate. By use of the definition of 1 unit (U) as the amount of enzyme that catalyzes 1 μM/min of 50 μM **2b**, purified human plasmin was calculated to have a specific activity of 1940 U/mg (Table 1). A similar serine protease,

Table 1. Activity of Human Plasmin and Human Cathepsin B Using 2b as a Substrate[a]

	plasmin (human)	cathepsin B (human)
specific activity (U/mg)	1940	1040
V_{max} (μM Dox/min)	3.76 ± 0.43	1.32 ± 0.06
K_M (μM)	171.10 ± 41.25	108.25 ± 12.47
turnover number (k_{cat}, s^{-1})	2.45 ± 0.46	0.49 ± 0.02
catalytic efficiency (M^{-1} s^{-1})	(1.43 ± 0.14) × 10^4	(4.59 ± 0.33) × 10^3

[a]Plasmin reactions were performed in PBS, pH 7.4, and cathepsin B reactions were performed in PBS containing 10 mM *N*-acetylcysteine (PBS-NAC), pH 6.5. One unit is defined as the hydrolysis of 1 μM **2b** per min.

trypsin, was chosen as a comparison to measure the specificity of the GaFK peptide toward plasmin. Reactions with bovine trypsin also readily produced dox, and a specific activity for bovine trypsin was calculated to be 4340 U/mg, indicating that serine proteases other than plasmin can activate **2b**.

While **2b** was specifically designed for activation by plasmin, there are members of other protease families that cut the C-terminal side of Phe-Lys sequences, and the enzyme cathepsin B is of particular interest because of its implication in the progression and poor prognosis for a variety of human cancers.[37−39] A prodrug that delivers dox upon cathepsin B cleavage following Phe-Lys has been described.[40,41] In initial experiments in PBS, human cathepsin B failed to demonstrate any HPLC-detectable production of dox. However, when 10 mM *N*-acetylcysteine was added to the PBS (PBS-NAC), which served to both acidify the buffer (to pH 6.5) and act as an activator by removing any small thiols that may have been blocking the active site cysteine of cathepsin B,[42−45] reactions between **2b** and the enzyme produced dox. The specific activity for purified human cathepsin B on **2b** was defined to be 1040 U/mg (Table 1). Under the same conditions as cathepsin B, papain, a cysteine protease derived from papaya and a representative member of the papain family of proteases, showed a specific activity of 890 U/mg (data not shown), suggesting that other members of the papain family in humans may also function to activate **2b**.

Michaelis−Menten kinetic experiments for the two human enzymes, plasmin and cathepsin B, were performed on substrate ranges from 10 to 400 μM using the same buffer conditions as above. Curve-fitting analyses (Table 1) demonstrated that the enzymes were similar in K_m (171 ± 41 μM for plasmin compared to 108 ± 12 μM for cathepsin B), but the calculated k_{cat} values ((2.45 ± 0.46 μM **2b**/s)/μM plasmin and (0.49 ± 0.02 μM **2b**/s)/μM cathepsin B) revealed that plasmin was 5-fold better at catalyzing the hydrolysis of **2b** than was cathepsin B. Additionally, plasmin was more than 3-fold more efficient than cathepsin B. The relatively low catalytic activity of cathepsin B was not due to significant deviation from an optimal condition, such as pH values closer to 5; in activity assays in which the PBS-NAC buffer was acidified with phosphoric acid to pH 5.5, cathepsin B was only 10% as active against **2b** as at pH 6.4 in standard PBS-NAC (data not shown), suggesting that our results at pH 6.5 may be indicative of the best activity of cathepsin B toward **2b**. These results indicate that serine proteases are better activators of **2b** than cysteine proteases but that tumors that have high levels of cathepsin B present in their microenvironments are still likely to be affected by **2b** treatment, even in the absence of plasmin, thereby broadening the spectrum of a potential proteolytically activated doxaz-based therapeutic regimen.

Plasma Stability of 2b. The activity of proteases in the bloodstream is hindered by the presence of α_2-macroglobulin and α_2-antiplasmins; therefore, **2b** should show little to no products of hydrolysis when incubated with human plasma. To demonstrate this, 50 μM **2b** was incubated for 24 h at 37 °C in plasma from healthy adult human donors. Periodically, samples were removed and analyzed for the appearance of dox and disappearance of **2b** by RP-HPLC and absorbance at 480 nm. To prevent damage to the analytical reverse phase column, the proteins were first removed by precipitation with ethanol. The results shown in Figure 4 indicate that **2b** levels in the supernatant do decrease with time, but a similar increase in dox is not observed, accounting for only approximately 9% of the total absorbance at 480 nm. Additionally, the loss of 480 nm absorbance from the prodrug was not distributed to other, unidentified red products but instead was lost from the total absorbance of the sample. This suggests that **2b** was incorporated into the pellet upon ethanol precipitation, likely through nonspecific binding to serum albumin, which is well-known as a drug carrier.[46,47] The lack of dox production indicates that, in human plasma, **2b** is very stable over 24 h and is unlikely to be prematurely activated.

Growth Inhibition of a Panel of Human Cancer Lines. Initial growth inhibition tests with **2b** were performed on MiaPaCa-2 and MCF-7 human cancer cell lines. As with **1b**, both cell lines responded equally well to prodrug alone, with log IC_{50} values in the range of −6.6 to −6.7 (Table 2). When co-treated with 0.2 U plasmin, the potency of the treatments increased by approximately 10-fold in each cell line, confirming that plasmin can mediate the release of doxaz from **2b**. As in the HPLC activity

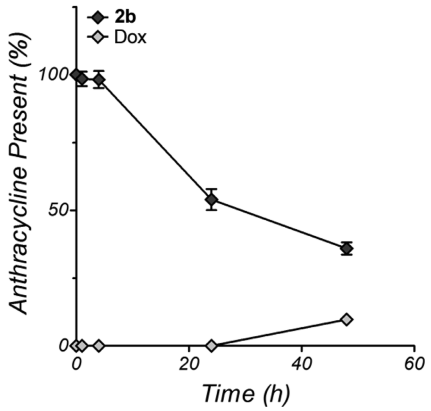

Figure 4. RP-HPLC analysis of the stability of **2b** in human plasma over 48 h. **2b** (50 μM) was incubated with undiluted human plasma from healthy individuals, and the time points were analyzed for the presence of all 480 nm absorbing species after precipitation of the protein fraction with absolute ethanol. Only **2b** (dark diamonds) and dox (light diamonds) were present. The points represent the mean ± the standard deviation of three measurements, and percentages are relative to the **2b** peak area present at the start of the experiment.

assays described above, co-treatment with bovine trypsin (0.2 U) reduced growth to a similar extent as plasmin, demonstrating that other serine proteases can easily activate **2b**. This has potential to be very beneficial, as many cancers have been found to have high levels of trypsin or trypsin-like serine protease activity.[48−51] Additionally, compared to treatment with **2b** alone, treatment with either cathepsin B or papain along with **2b** resulted in increased growth inhibition in both cell lines. However, this was significantly less than the growth inhibition mediated by **2b** activated by either serine protease. These results further indicate that serine proteases are more effective at activating **2b**. When proteolytic activity is inhibited with either 5 μM aprotinin to inhibit serine proteases or Roche's Complete protease inhibitor cocktail (made to 1× according to the manufacturer's instructions), the reduction in cellular response to **2b** is apparent but not significant. This may be due to constant secretion of active proteases by the cell, which effectively overwhelms the limited amount of added inhibitor, since the potency of the inhibitors was verified by their ability to prevent the increase in potency of a **2b**−plasmin co-treatment over **2b** treatment alone (data not shown). However, the inability of high concentrations of protease inhibitors to protect cells could also could indicate that there are alternative mechanisms of activation beyond those probed in this study. These alternative mechanisms will be the subject of future studies and characaterization of **2b**.

The results presented above indicate that **2b** may be activated by both serine and cysteine proteases; in a mixed protease environment, as is likely present at a tumor, plasmin and related serine proteases will play a larger role in activation of **2b** than will cysteine proteases. Therefore, a panel of cancer cell lines was tested with **2b** alone and **2b** + 0.2 U exogenous human plasmin. As shown in Table 3, we tested four pancreatic cancer lines (BxPC3, L3.3, L3.5, and L3.6PL), a small cell lung cancer line (SHP77), and an ovarian cancer line (NCI-RES/Adr). The last two lines, SHP77 and NCI-RES/Adr, are resistant to dox but are sensitive to doxaz treatment.[11] Finally, we tested a noncancer derived, but uPA-rich, human cell line, HEK-293T. Among the cancer cell panel, the average log IC_{50} was −6.3, with a range from −5.8 in the SHP77 to −6.65 in the L3.5. The growth of the nontumor HEK-293T line was inhibited to approximately the same extent as the cancer lines with either treatment condition. This is in line with observations that this cell line expresses a particularly high level of uPA, a serine protease that converts plasminogen into plasmin.[52] Given that at least two different serine protease enzymes can catalyze the hydrolysis of **2b**, it is plausible that other enzymes with related activity, such as uPA and tissue plasminogen activator (tPA), could exhibit at least low level catalysis of **2b**. Since tumors often overexpress multiple members of proteolytic pathways, while normal tissues tightly control protease activity, the broad specificity of **2b** may allow for a more tunable therapeutic; an efficacious dose for a very uPA/plasmin-heavy tumor may be different from an equivalently efficacious dose for a cathepsin B-heavy tumor. The proteolytic profile contributed by invading endothelial cells during active angiogenesis may allow for further distinction between tumor and normal tissues, thereby potentially allowing doses to be reduced to achieve the same antitumor effect with fewer side effects and tissue toxicities.

Table 3. Growth Inhibition of a Panel of Cell Lines by 24 h Treatment with 2b with or without 0.2 U of Human Plasmin, Represented by the IC_{50} in log *M* Units[a]

	2b alone	**2b** + plasmin (0.2 U)
BxPC3	−6.0 ± 0.1	−7.4 ± 0.1
L3.3	−6.6 ± 0.1	−8.40 ± 0.07
L3.5	−6.65 ± 0.04	−8.58 ± 0.04
L3.6PL	−6.50 ± 0.08	−8.50 ± 0.04
SHP77[b]	−5.80 ± 0.03	−7.53 ± 0.05
NCI-RES/Adr[b]	−6.04 ± 0.05	−7.93 ± 0.05
cancer cell mean	−6.3 ± 0.3	−8.1 ± 0.5[d]
HEK-293T[c]	−6.7 ± 0.1	−8.52 ± 0.04

[a]BxPC3, L3.3, L3.5, and L3.6PL are pancreatic cancer. SHP77 are small-cell lung cancer, and NCI-RES/Adr are ovarian cancer cells. The last two lines are dox-resistant. HEK-293T cells are non-tumor-derived human embryonic kidney cells. Values for individual cell lines are the mean ± standard error of at least 12 measurements. The values for cancer cells were averaged and are shown in the "cancer cell mean" row ± the standard deviation. [b]Doxorubicin resistant. [c]Non-tumor-derived. [d]$P < 0.0001$ relative to **2b** alone.

Cellular Uptake. The presumed activation scheme for **2b** utilizes external activation by secreted proteases, followed by cellular uptake of the active doxaz cytotoxin. However, it is

Table 2. Growth Inhibition of MCF-7 and MiaPaCa-2 Cells by 24 h Treatment of 2b with Various Activators and Inhibitors[a]

		activation				inhibition	
	2b alone	**2b** + plasmin (0.2 U)	**2b** + trypsin (0.2 U)	**2b** + papain (0.2 U)	**2b** + cathepsin B (0.2 U)	**2b** + aprotinin (5 μM)	**2b** + Complete protease inhibition (1×)
MiaPaCa-2	−6.6 ± 0.2	−7.63 ± 0.03	−7.58 ± 0.04	−7.16 ± 0.03	−6.80 ± 0.08	−6.55 ± 0.06	−6.4 ± 0.2
MCF-7	−6.7 ± 0.1	−7.57 ± 0.02	−7.5 ± 0.1	−7.22 ± 0.05	−6.92 ± 0.09	−6.53 ± 0.04	−6.6 ± 0.3

[a]IC_{50} values are reported as log *M*, and the value of U is defined as the hydrolysis of 1 μM **2b** per min.

dx.doi.org/10.1021/jm300714p | J. Med. Chem. 2012, 55, 6595−6607

possible that some fraction of **2b** may cross the plasma membrane and be activated internally. Although there is likely to be far fewer intracellularly active proteases relative to the potential activity of external proteases at a tumor site, several cellular processes require proteolytic pathways, particularly proteosome and lysosomal protein degradation pathways. To test for cellular uptake of **2b**, MCF-7 and MiaPaCa-2 were treated with either 0.5 μM **2b** alone or co-treatments of 0.5 μM **2b** and 0.2 U plasmin for up to 5 h. The cells were then analyzed by flow cytometry for the anthracycline fluorophore. Uptake of **2b** alone is characterized by a fast initial increase in fluorescence, up to 1.8-fold over background, followed by a slower increase to approximately 2- to 2.5-fold over background for the rest of the period (Figure 5), likely representing a baseline rate of hydrolysis

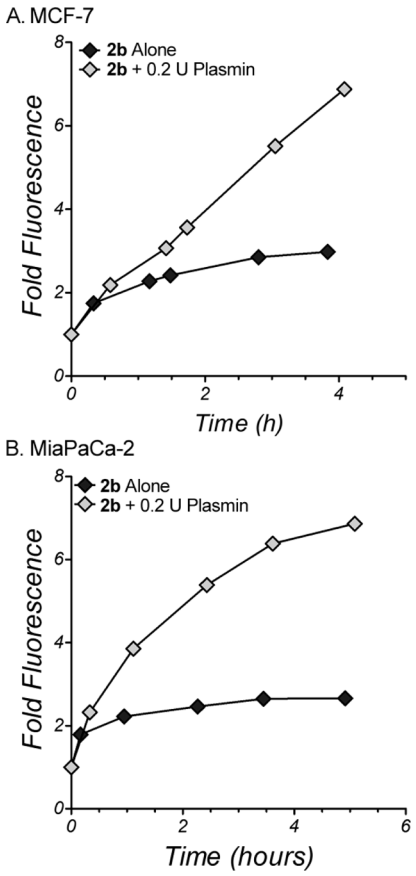

Figure 5. Uptake of **2b** with or without plasmin into human cancer cells. An amount of 250 000 cells per well of either MCF-7 (A) or MiaPaCa-2 (B) was treated with 0.5 μM **2b** alone (dark diamonds) or 0.5 μM **2b** with 0.2 U human plasmin (light diamonds) for various time periods and analyzed by flow cytometry for the presence of fluorescence due to the anthracycline fluorophore and compared to the fluorescence of untreated cells. Data representative of repeated measurements (at different time points) are shown here, with variation of approximately 10−20% between the experiments.

of **2b** to release the highly permeable doxaz by cell-secreted proteases. When exogenous plasmin is added, the cellular fluorescence is much greater, approaching 7-fold over background by 4−5 h, presumably reflecting the increased abundance of cell-permeable doxaz. Although the difference in cellular fluorescence between the co-treatment and treatment with only **2b** is not particularly dramatic (approximately 3-fold), this level can have a demonstrable difference in toxicity. As previously shown, this ratio of uptake difference, observed between dox-sensitive SK-HEP-1 liver carcinoma cells and dox-resistant NCI-RES/Adr (formerly MCF-7/Adr) cells, results in cytotoxic responses that differ by about 1.3−1.5 orders of magnitude.[13] While future studies will provide a better characterization, such as a description of the fast but small initial increase in fluorescence of cells in response to **2b** without exogenous plasmin, these data suggest that intact **2b** is poorly taken up by cancer cells but that upon activation, liberated doxaz readily crosses the membrane. Therefore, it is unlikely that high levels of **2b** activation will occur by intracellular proteolytic pathways, reducing the likelihood for side effects and toxicities to normal tissues and organs.

CONCLUSIONS

The aim of this research was to produce a high-potency, broad spectrum antitumor prodrug to deliver our powerful cytotoxin doxaz. Release of doxaz in this design is mediated by proteolytic hydrolysis, as compared to our previous work with a CES2-activated doxaz prodrug, which has shown promise but is likely a narrow spectrum prodrug.[15] Our first design of a proteolytically released doxaz prodrug was based upon previously published work on dox but was limited in its development potential by a persistent epimerization of the terminal non-natural D-alanine. This is unlikely to have any directly detrimental effects on endopeptidase-specific hydrolysis of the Lys-*p*-aminobenzylamide bond. However, the loss of the non-natural isomer at the N-terminus may increase the susceptibility of the prodrug to degradation by aminopeptidase activity.[53] This could result in poorer plasma stability of the intact prodrug, but perhaps more importantly, it changes the peptidyl substrate. This could result in unknown catalytic hydrolysis rates from our targeted enzymes, which may change the profile of activating proteases and potentially introduce a host of side effects that may otherwise not be present in therapy with this prodrug. However, using the small amounts of isomerically pure **1b**, we were able to demonstrate that additional efforts to improve the design and synthesis of a protease-activated doxaz prodrug were warranted. Plasmin-induced cleavage of **1b** was fast and robust, and there was a significant advantage in cytotoxic activity by using doxaz as the warhead instead of dox. Therefore, having evidence that a doxaz prodrug containing the aFK sequence was a promising core for a protease-activated prodrug, we directed our efforts at producing a more scalable version that avoided the epimerization problems of **1b**.

A more successful scalable design incorporated *N*-acetyl glycine at the amino terminus of the peptidyl chain. **2b**, unlike **1b**, exhibited no evidence of epimerization at any point in the synthetic process and maintained good kinetics of activation by plasmin and stability in human plasma. **2b** was a good substrate for plasmin but could also be hydrolyzed by the related serine protease trypsin, as well as members of the papain family, specifically papain and human cathepsin B. This multienzyme characteristic of **2b** adds to the spectrum of tumor profiles against which it could be beneficial, particularly in the case of cathepsin B, but also suggests that enzymes with trypsin-like serine protease activity, such as the tumor-associated enzyme uPA, can also contribute to activation. Antitumor activity alone was good and was enhanced by the addition of exogenous enzymes. Importantly, **2b** was active against SHP77 and NCI-RES/Adr cells, both of which are resistant to dox and sensitive to doxaz. Finally, although most normal cells possess some proteolytic activity, particularly in the lysosomal compartment, unactivated **2b** is unlikely to be highly toxic because of its limited membrane

permeability. Therefore, the majority of the release of doxaz is expected to occur externally because of secreted proteases, the expression of which has been consistently linked to highly invasive, angiogenic tumor environments.[21,22]

MATERIALS AND METHODS

General. Clinical samples of doxorubicin hydrochloride formulated with lactose were gifted by FeRx (Aurora, CO). Unless otherwise noted, all reagents and amino acids for solid-phase peptide synthesis were purchased from Nova Biosciences (La Jolla, CA) and other chemicals and reagents were acquired from Aldrich (Milwaukee, WI). Analytical HPLC was performed on Agilent 1050/1100 hybrid instruments equipped with a 1050 series autoinjector, a 1100 series UV/visible diode array detector, and a 1046A fluorescence detector (Santa Clara, CA). An Agilent Zorbax octadecylsilyl (C18) reverse phase column (4.6 mm i.d. × 150 mm, 5 μm) was used for chromatography. Unless specifically indicated, elution was performed at 1 mL/min and room temperature with gradients of acetonitrile and 20 mM sodium phosphate buffer, pH 4.6, containing 0.02% sodium azide. Method 1 had acetonitrile percentages of 20% from 0 to 1.5 min, 30% at 5 min, 80% from 15 to 20 min, and 20% at 24 min. Method 2 consisted of acetonitrile percentages: 20% to 40% from 0 to 5 min, 50% from 8 to 9 min, and 20% at 11 min. The presence of anthracycline-containing molecules was monitored by absorbance at 480 nm, and retention times are noted individually. All NMR spectra were taken at 400 or 500 MHz on a Varian Unity INOVA spectrometer (Palo Alto, CA) or a Bruker-Avance III 300 MHz spectrometer (Billerica, MA) in deuterated solvents from Cambridge Isotope Laboratories, Inc. (Andover, MA). Chemical shifts are reported in δ values of ppm and were standardized by the residual solvent peak in MestReNova NMR software (Mestrelab Research, Santiago de Compostela, Spain). The purity of all characterized compounds was verified to be at least 95% by using a combination of HPLC (monitoring wavelengths of 230, 260, 280, 300, 400, and 480 nm) and NMR. UV−vis spectroscopy was performed on a Hewlett-Packard/Agilent 8452A diode array instrument. Electrospray mass spectra were obtained with a Perkin-Elmer Sciex API III$^+$ (Waltham, MA) or ABI Pulsar QqT high resolution instrument (Foster City, CA), equipped with an ion-spray source at atmospheric pressure. Purification by radial chromatography was done with a Harrison Research model 7924T Chromatotron (Palo Alto, CA). Analysis by flow cytometry was performed with a Becton-Dickinson Biosciences FACscan (San Jose, CA), and a PowerWave X plate reader (BIO-TEK Instruments, Winooski, VT) was used for analyzing 96-well plate growth inhibition assays.

General Tissue Culture. All tissue culture reagents were acquired from Gibco Life Sciences (Grand Island, NY) and plates from Sarstedt, Inc. (Newton, NC) or Corning, Inc. (Corning, NY) unless otherwise noted. All cells were acquired from the American Type Culture Collection (Rockville, MD) except NCI/RES-Adr (a gift from William Wells, Michigan State University, East Lansing, MI), L3.3, L3.5, and L3.6PL (all gifts of Wells Messersmith, University of Colorado, Anschutz Medical Campus, Denver, CO). NCI/RES-Adr and SHP77 were maintained in RPMI-1640, supplemented with 10% (v/v) fetal calf serum and 1% (v/v) pencillin−streptomycin stock solution. MCF-7, MiaPaCa2, BxPC3, L3.3, L3.5, L3.6PL, and the nontumor-derived HEK-293T were grown in Dulbecco's modified essential medium (DMEM) containing the same above supplements in the same concentrations. All of the above cells were grown in a humidified incubator under an atmosphere of 5% CO_2/95% air at 37 °C.

Synthesis. The synthesis of the final compound, **2**, is described below, while the synthesis of the initial design, **1**, can be found in Supporting Information. The water miscible solvents, tetrahydrofuran (THF) and DMSO, were made dry by distillation from Na^0/benzophenone and storage over 4 Å molecular sieves, respectively.

Doxorubicin Free Base from Clinical Samples. Lyophilized pellets of expired clinical samples of doxorubicin HCl (20−50 mg) containing 100−250 mg of lactose monohydrate (Bedford Laboratories, Bedford, OH) were dissolved in methanol to a final concentration of 2 mg/mL and combined in a separatory funnel. The methanol solution was diluted with 100 mM sodium phosphate buffer, pH 8.5, for a final concentration of 0.4 mg/mL dox−HCl as a mixture of precipitated and solubilized material. The free base of dox was extracted from the solution by two washes with equal volumes of chloroform, leaving almost no red color in the aqueous fraction. The chloroform was dried with anhydrous sodium sulfate, filtered, and removed by rotary evaporation to yield a red solid. The solid was dried thoroughly under high vacuum (10^{-2} Torr) for at least 2.5 h to yield pure dox free base in a final yield of 98%, as indicated by optical density at 480 nm and a molar extinction coefficient of 11 500 M^{-1} cm^{-1} in 75% DMSO/25% water.

Doxazolidine. Dox free base was dissolved to a final concentration of 5−10 mg/mL in deuteriochloroform, and 1.1−2 equiv of prilled paraformaldehyde (Aldrich, Milwaukee, WI) was added. The reaction mixture was monitored by ^{1}H NMR, with complete consumption of dox occurring after 2−3 days, as evidenced by the appearance of the doxaz−methylene AX pattern at 4.31 and 4.68 ppm and doxf AX pattern at 4.21 and 4.73 ppm in the ^{1}H NMR spectrum. Loss of dox was evident by the dox-specific aromatic triplet pattern for the proton at the 2-position, which appears at 7.81 ppm (compared to 7.78 for doxaz and 7.70 for doxf). The amount of paraformaldehyde added determines the doxaz/doxf ratio, since doxaz reacts with an additional equiv of formaldehyde to form doxf. Complete assignments of the ^{1}H NMR spectra for doxaz and doxf have been published.[10] The reaction mixture was then filtered and the deuteriochloroform removed by rotary evaporation. The doxaz/doxf mixture was used without further purification, since doxf readily hydrolyzes to produces 2 equiv of doxaz.

Fmoc-*p*-aminobenzyl Alcohol (Fmoc-PABA, 3). *N*-(Fluorenylmethyloxycarbonyloxy)succinimide (*N*-Fmoc-*N*-hydroxysuccinimide, 6.0 g, 17.8 mmol) in *p*-dioxane (60 mL) was added dropwise to *p*-aminobenzyl alcohol (PABA, 2.5 g, 20.5 mmol) in *p*-dioxane (30 mL). After the mixture was stirred for 48 h, 90 mL of deionized H_2O was added and the desired product immediately precipitated. The product was isolated by filtration and washed 4 times with deionized H_2O (60 mL). The isolated Fmoc-PABA (5.9 g, 95%) showed the following spectral properties: ^{1}H NMR ($CDCl_3$) δ 4.26 (t, 1H, J = 7 Hz, Fmoc-CH), 4.53 (d, 2H, J = 7 Hz, Fmoc-CH_2), 4.63 (s, 2H, PABA-CH_2), 6.62 (bs, 1H, NH), 7.30 (t, 2H, J = 7 Hz, Fmoc), 7.34 (d, 2H, J = 7 Hz, PABA), 7.36 (b, 2H, PABA), 7.40 (t, 2H, J = 7 Hz, Fmoc), 7.60 (d, 2H, J = 7 Hz, Fmoc), 7.77 ppm (d, 2H, J = 7 Hz, Fmoc); ESI-MS, observed m/z = 384.1014; calculated m/z for ($M + K^+$) = 384.0996.

Loading of Fmoc-PABA to 2-Chlorotrityl Resin. Fmoc-PABA (2 equiv) was added to 1.0 g of 2-chlorotrityl chloride polystyrene resin in 10 mL of dry THF followed by 4 equiv of dry pyridine. The solution was stirred and heated at 60 °C in an oil bath for 16 h under argon. The solution was filtered through a coarse sintered glass frit, and the resin was washed with DCM/MeOH/DIEA, 17:2:1 mL (3×), followed by 10 mL of DCM (2×), 10 mL of DMF (2×), 10 mL of DCM (3×). The resin was dried under high vacuum (10^{-2} Torr) overnight and then checked for loading level according to previously published methods.[54]

Solid Phase Peptide Synthesis. The peptide was synthesized by the solid phase method using the Fmoc strategy starting with preloaded Fmoc-PABA. The peptide was prepared on a 0.25 mmol scale by single amino acid couplings using a 4-fold excess of *N*-acetyl-Gly and the Fmoc-protected amino acids D-Ala (Chem-Impex, International, Wood Dale, IL), L-Phe, and L-Lys-alloc. Activation was done with 2-(1*H*-benzotriazole-1-yl)-1,1,3,3-tetramethyluronium hexafluorophosphate (HBTU)/*N*-hydroxybenzotriazole (HOBT), and the synthesis was performed on an ABI 433A peptide synthesizer (Applied Biosystems, Carlsbad, CA). Owing to the poor nucleophilicity of the aniline nitrogen of PABA, the coupling of the first amino acid, Fmoc-Lys(alloc), required an extended coupling time by modifying the software instructions to vortex the reaction for 60 s, then allow it to sit for 10 min. This cycle was repeated 88 times. Fmoc groups were removed by sequential treatment (3×) with 20% piperidine/DMF, and all other amino acid couplings followed standard conditions, to yield Ac-Gly-D-Ala-L-Phe-L-Lys(alloc)-PABA (Ac-GaFK(alloc)-PABA) coupled to the polystyrene resin.

Cleavage of Ac-GaFK(alloc)-PABA (8) from the Resin and Activation to Ac-GaFK(alloc)-PABA-pNP Carbonate (9). The resin was placed into a medium-grain fritted funnel and washed twice with DCM (20 mL). Pyridine/MeOH (10% v/v, 20 mL) was added to the

receiving flask to protect the peptide after cleavage. TFA/DCM (2% v/v, 10 mL) was then added and swirled for 1 min. The mixture was then gently vacuum filtered without allowing the resin to proceed to dryness. This step was repeated 3 times followed by a 20 mL DCM wash. The filtrate contained the peptide and pyridinium trifluoroacetate salt and was rotary-evaporated to ~10% of the original volume. Approximately 40 mL of deionized water was added to the flask, and the solution was allowed to cool in an ice bath for at least 10 min. The precipitate was collected on a fritted funnel and washed with 10 mL of deionized water (3×), followed by 10 mL of diethyl ether (2×). An oven-dried round-bottom flask equipped with a magnetic stir bar was cooled under argon and charged with 25.0 mL of dry THF and **8** (376.6 mg, 0.577 mmol). To the stirring suspension, *p*-nitrophenyl chloroformate (127.9 mg, 1.1 equiv) was added followed immediately by pyridine (51.33 μL, 1.1 equiv). Over the course of 20 min, all solids went into solution, after which the reaction progress was monitored by RP-HPLC (method 1) until complete, as evidenced by the consumption of **8** (eluting at 13.4 min), which typically required 18−24 h. The reaction mixture was then diluted with 250 mL of ethyl acetate and washed once with 150 mL of deionized water, followed by extractions with 150 mL of saturated sodium bicarbonate until the aqueous layer no longer turned yellow (typically five extractions). The organic layer was dried over sodium sulfate and concentrated by rotary evaporation to yield 400 mg (85%) of a pale yellow solid that was used without further purification. Ac-GaFK(alloc)-PABA-pNP was characterized by the following spectroscopic data with NMR assignments made from ^{1}H NMR and homonuclear COSY (DMSO-d_6, 500 MHz): δ 0.94 (d, 3H, J = 7.0 Hz, Ala-CH_3), 1.32−1.27 (m, 1H, Lys-γ'), 1.40−1.33 (m, 1H, Lys-γ), 1.49−1.40 (m, 2H, Lys-δ), 1.70−1.61 (m, 1H, Lys-β'), 1.77−1.71 (m, 1H, Lys-β), 1.82 (s, 3H, *N*-acetyl), 2.75 (dd, 1H, J = 13.7, 10.7 Hz, Phe-β), 2.98 (apparent q, 2H, J = 6.3 Hz, Lys-ε), 3.09 (dd, 1H, J = 13.7, 3.5 Hz, Phe-β'), 3.62 and 3.66 (AB of ABX pattern, 2H, J_{AB} = 16.5, J_{AX} = 5.8, J_{BX} = 5.7 Hz, Gly-α), 4.24 (apparent p, 1H, J = 7.0 Hz, Ala-α), 4.35 (apparent q, 1H, J = 7.7 Hz, Lys-α), 4.43 (d, 2H, J = 5.3 Hz, alloc), 4.56 (ddd, 1H, J = 10.7, 8.6, 3.5 Hz, Phe-α), 5.14 (dd, 1H, J = 10.6, 3.0 Hz, alloc), 5.25 (s, 2H, Bn), 5.88 (ddt, 1H, J = 17.0, 10.6, 5.3 Hz, alloc), 7.18−7.12 (m, 1H, *p*-Ph), 7.29−7.18 (m, 5H, *o*,*m*-Ph and Lys-ε-NH), 7.42 (d, 2H, J = 8.5 Hz, PABC-$H_{2,6}$), 7.60−7.53 (AA′XX′ pattern, 2H, PNP-$H_{2,6}$), 7.67 (d, 2H, J = 8.5 Hz, PABC-$H_{3,5}$), 8.00 (d, 1H, J = 7.3 Hz, Ala-α-NH), 8.04 (X of ABX, 1H, J_{AX} = 5.8, J_{BX} = 5.7 Hz, Gly-α-NH), 8.22 (d, 1H, J = 7.4 Hz, Phe-α-NH), 8.24 (d, 1H, J = 6.2 Hz, Lys-α-NH), 8.36−8.28 (AA′XX′ pattern, 2H, PNP-$H_{3,5}$), 10.05 (s, 1H, PABC-NH) ppm.

Ac-GaFK(alloc)-PABC-Doxaz (10). An oven-dried round-bottom flask equipped with a magnetic stir bar was cooled under argon and charged with **9** (126.13 mg, 0.1161 mmol), 1-hydroxybenzotriazole (23.61 mg, 1 equiv), and 500 μL of dry DMSO. To this, doxaz (85.68 mg, 1 equiv) dissolved in 500 μL of dry DMSO was added, and the mixture was left to stir under argon in the dark and monitored by HPLC (method 1) until complete, as evidenced by the disappearance of carbonate starting material (approximately 36 h). The reaction mixture was then diluted with an additional 2 mL of DMSO. A 15 mL medium fritted sintered glass funnel was charged with 10 mL of cold PBS, pH 7.4. The red reaction mixture was added dropwise, and the resulting red precipitate was washed four times with 10 mL of PBS and then two washes with 10 mL of deionized water. The precipitate was washed from the filter with a mixture of 10:1 chloroform/methanol and concentrated by rotary evaporation. The majority of the crude red solid, which was a mixture containing a 46% yield of **10**, was moved forward without any additional purification. However, to facilitate characterization of **10**, the red solid was purified by preparative silica gel TLC, spotted in and eluted with 10:1 chloroform/methanol. The desired product (the major band) was excised, suspended, and vortexed in the elution solvent and centrifuged to remove the silica gel. The solvent was removed by rotary evaporation to produce solid, pure **10** that was characterized by the following spectroscopic data with NMR assignments made from ^{1}H NMR, homonuclear COSY, ROESY, HSQC, and HMBC spectra: ^{1}H NMR at 55 °C (500 MHz, $CDCl_3$) δ 1.20 (d, 3H, J = 7 Hz, Ala-Me), 1.31 (d, 3H, J = 5 Hz, 5′-Me), 1.32 (m, 2H, Lys-γ), 1.44 (m, 1H, Lys-δ), 1.50 (broad m, 1H, Lys-δ), 1.73 (m, 1H, Lys-β), 1.75 (m, 1H, 2′), 1.87 (m, 1H, Lys-β), 1.88 (s, 3H, Ac), 2.1 (dd, 1H, J = 14, 4 Hz, 8), 2.17 (broad m, 1H, 2′), 2.41 (d, 1H, J = 14, Hz, 8), 3.01 (d, 1H, J = 18 Hz, 10), 2.98 (dd, 1H, J = 9, 5 Hz, Phe-β), 3.09 (m, 2H, Lys-ε), 3.23 (m, 1H, Phe-β), 3.23 (d, 1H, J = 18 Hz, 10), 3.98 (dd, 1H, J = 5, 1 Hz, 4′), 4.03 (s, 3H, 4-OMe), 4.10 (m, 1H, Ala-α), 4.08−4.12 (m, 2H, 3′ and 5′), 4.45 (dd, 1H, J = 9, 5 Hz, Lys-α), 4.49 (broad, 2H, 3‴), 4.55 (dd, 1H, J = 9, 6 Hz, Phe-α), 4.70 (s, 2H, 14), 4.90 (d, 1H, J = 4 Hz, OCH_2N), 4.96 (broad, 1H, OCH_2N), 5.06 and 5.8 (broad AB pattern, 2H, J = 11 Hz, Bn), 5.14 (d, 1H, J = 10 Hz, 1‴c ROESY), 5.23 (d, 1H, J = 18 Hz, 1‴t ROESY), 5.26 (m, 1H, 7), 5.39 (t, 1H, J = 5 Hz, 1′), 5.85 (ddt, 1H J = 16, 10, 5 Hz, 2‴), 7.15 (m, 1H, Phe-*p*-Ph), 7.16 (m, 2H, Phe-*o*-Ph), 7.22 (m, 2H, Phe-*m*-Ph), 7.26 (d, 2H, J = 8 Hz, 2″ ROESY), 7.37 (d, 1H, J = 8 Hz, 3), 7.56 (d, 2H, J = 8 Hz, 3″), 7.74 (t, 1H, J = 8 Hz, 2), 7.99 (d, 1H, J = 8 Hz, 1); ^{13}C NMR chemical shifts from HSQC δ 15.75 (5′-Me), 16.19 (Ala-Me), 22.25 (Ac), 22.54 (Lys-γ), 29.11 (Lys-δ), 29.27 (2′), 30.49 (Lys -β), 34.09 (10), 36.73 (Phe-β), 35.84 (8), 40.33 (Lys-ε), 42.79 (Gly-α), 49.83 (Ala-α), 53.68 (Lys-α), 55.16 (Phe-α), 56.59 (4-OMe), 65.05 (14), 65.33 (3′ and 5′), 65.61 (3‴), 66.79 (Bn), 68.95 (7), 77.60 (4′), 78.83 (O-CH_2-N), 99.59 (1′), 117.29 (1‴), 118.97 (3), 119.76 (1), 120.11 (3″), 126.88 (*p*-Phe), 128.81 (*o*-Phe), 128.79 (2″), 128.52 (*m*-Phe), 132.79 (2‴), 135.54 ppm (2); some unprotonated carbons from HMBC δ 121.7 (4a), 133.8 (6a), 161.5 (4), 170.5 (Lys-α CO), 171.8 (Ac-CO), 170.8 (Gly-CO), 171.9 (Phe-CO), 173.7 (Ala-CO), 213.9 ppm (13); MS-ESI$^+$, observed MH^+ 1234.4832; calculated MH^+ 1234.4827.

Deprotection To Form GaFK-Doxaz, Phosphate Salt (2b). Compound **10** (5.3 mg, 0.0043 mmol) was dissolved in 600 μL of 5:1 DCM/AcOH. To this, tetrakis(triphenylphosphine)Pd^0 (4.96 mg, 1 equiv, Strem Chemicals, Newburyport, MA) was added. The reaction was left in the dark for 80 min, at which point the DCM was removed by rotary evaporation. The acidic solution was diluted with 6 mL of 20 mM phosphate buffer, pH 4.6, and extracted 3 times with 6−7 mL of ethyl acetate to remove any triphenylphosphine oxide produced during the deprotection, spinning briefly at 1500*g* to produce a clean interface. The desired product was purified from the extracted aqueous solution by preparative HPLC on a C-18 Dyanmax 100 Å, 25 cm semipreparatory column (10 mm i.d.) run isocratically with 50% acetonitrile, 50% 20 mM phosphate buffer, pH 4.6, at 3 mL/min. The product eluted at 10 min. The eluent was lyophilized to yield a red solid consisting of a mixture of the final material and sodium phosphate in 95% overall yield from **9**. The prodrug was dissolved away from the majority of the sodium phosphate by five washes with 50 μL of 9:1 DMSO/water to yield an acidic water−DMSO solution of **2b**. Cold storage (>3 weeks at −20 °C) of **2b** in this form eventually resulted in multiple red products by HPLC, presumably due to a low level reactivity of DMSO with the small percentage of deprotonated Lys-ε-NH_2. To prevent this, following removal of the majority of the phosphate salts, the DMSO was evaporated by SpeedVac (10^{-2} Torr) and the pure final material dissolved in saline (0.9% NaCl) containing 10% PEG-400. To increase the stability of the product, 5 mM sodium phosphate, pH 4.6, was added to this solution. Cold storage of this formulation has shown good stability for at least 2 months. The overall yield of the formulated final **2b** was 78% from **9** and was characterized by the following spectroscopic data with NMR assignments made from ^{1}H NMR, homonuclear COSY, ROESY, HSQC, and HMBC spectra: ^{1}H NMR at 50 °C (500 MHz, DMSO-d_6/D_2O phosphate, pH 4) δ 1.01 (d, 3H, J = 7 Hz, Ala-Me), 1.17 (d, 3H, J = 7 Hz, 5′-Me), 1.24−1.42 (broad m, 2H, Lys-δ), 1.55 (p, 2H, J = 8 Hz, Lys-γ), 1.6−1.76 (broad m, 2H, Lys-β), 1.84 (m, 2H, 2′), 1.83 (s, 3H, Ac), 2.13 (dd, 1H, J = 14, 5 Hz, 8), 2.18 (dd, 1H, J = 14, 3 Hz, 8), 2.75 (m, 2H, Lys-ε), 2.89 and 2.91 (AB pattern, 2H, J = 18 Hz, 10), 2.79 (m, 1H, Phe-β), 3.04 (m, 1H, Phe-β), 3.97 (dd, 1H, J = 6, 2 Hz, 4′), 4.14 (q, J = 6 Hz, 1H, Ala-α), 3.93 (s, 3H, 4-OMe), 4.04 (q, J = 6 Hz, 1H, 3′), 4.24 (m, 1H, 5′), 4.26 (m, 1H, Lys-α), 4.42 (dd, 1H, J = 11, 2 Hz, Phe-α), 4.54 and 4.55 (AB pattern, J = 20 Hz, 2H, 14), 4.82 and 4.83 (AB pattern, 2H, J = 3 Hz, OCH_2N), 4.95 (dd, J = 5, 3 Hz, 1H, 7), 4.99 and 5.01 (AB pattern, 2H, J = 13 Hz, Bn), 5.22 (t, 1H, J = 4 Hz, 1′), 7.10 (broad m, 1H, Phe-p-Ph), 7.16 (broad m, 4H, Phe-*o*- and *m*-Ph), 7.25 (d, 2H, J = 7 Hz, 2″ ROESY), 7.37 (d, 1H, J = 8 Hz, 3), 7.51 (broad, 2H, 3″), 7.56 (m, 1H, 2), 7.84 (m, 2H, 1 and 3); ^{13}C NMR chemical shifts from HSQC δ 16.15 (5′-Me), 17.76 (Ala-Me), 22.50 (Ac), 26.57 (Lys-γ), 22.57 (Lys-δ), 29.27 (2′),

dx.doi.org/10.1021/jm300714p | J. Med. Chem. 2012, 55, 6595−6607

30.99 (Lys-β), 32.47 (10), 37.15 (Phe-β), 36.95 (8), 48.82 (Lys-ε), 42.37 (Gly-α), 48.86 (Ala-α), 49.7 (3′), 53.99 (Lys-α), 54.58 (Phe-α), 56.91 (4-OMe), 63.86 (14), 64.20 (5′), 66.40 (Bn), 69.85 (7), 77.45 (4′), 78.25 (O-CH_2-N), 99.49 (1′), 11.46 (1 and 3), 120.03 (3″), 129.37 (Phe-*p*- and *o*-Ph), 128.61 (2″), 128.52 (Phe-*m*-Ph), 135.54 ppm (2); some unprotonated carbons from HMBC δ 75.58 (9), 119.78 (12a), 135.18 (4a), 134.56 (6a), 161.39 (4), 161.42 (12), 171.73 (Ac-CO), 170.20 (Gly-CO), 171.9 (Phe-CO), 173.15 (Ala-CO), 214.12 ppm (13); MS-ESI$^+$, observed MH^+ 1150.4590; calculated MH^+ 1150.4615.

In Vitro Assays. HPLC Activity Assays. Assays to determine the activities of various enzymes toward protease-cleavable doxaz prodrugs were performed as a two-pronged measurement: a hydrolysis time course to assess the activity of each enzyme stock on **2b** and a Michaelis−Menten kinetic analysis to assign kinetic values for the activity of human-derived enzymes on **2b**. Time course experiments were conducted at 37 °C by incubating 50 μM prodrug with varying concentrations of either plasmin (EMD Biosciences, La Jolla, CA) or trypsin (Research Products International, Mt. Prospect, IL) in PBS. Reactions with cathepsin B (Enzo Biosciences, Ann Arbor, MI) and papain (Sigma, Milwaukee, WI) were performed by first diluting the enzymes 2-fold in PBS-NAC (PBS with 10 mM *N*-acetylcysteine), followed by reaction with 50 μM **2b** in either PBS-NAC, pH 6.5, or PBS-NAC, pH 5.5, at 37 °C. At various times, 50 μL of the reaction mixture was added to an equal volume of absolute ethanol to quench the reaction. The collected samples were stored at −20 °C for at least 2 h and then centrifuged at 15000*g* for 5 min to precipitate the protein. The supernatant was analyzed by RP-HPLC (method 2), monitoring the loss of the starting material (elution at 8−9 min) and accumulation of dox (elution at 4−5 min). The fraction dox was converted into micromolar concentration and fit with a one-phase exponential association curve by nonlinear least-squared analysis (GraphPad Prism 5.0, GraphPad Software, Inc., La Jolla, CA). To calculate an activity for each enzyme, only those points that produced less than 20% dox during the reaction were analyzed to limit the analysis to those points in which the reaction rate was approximately linear with time. The selected points were fit with linear least-squared analysis, and the slope of the line was used to calculate the activity of the enzymes on **2b**. One unit was defined as the amount of enzyme required to hydrolyze 1 μM prodrug per min under these conditions (37 °C and 50 μM prodrug in buffer, either PBS or PBS-NAC).

Michaelis−Menten kinetic analyses were carried out for human plasmin and human cathepsin B, using **2b** as a substrate and the buffer conditions described above. A range of concentrations from 10 to 400 μM was made in buffer and enzyme to a final volume of 60 μL. The final enzyme amounts were 0.2 U plasmin and 0.08 U cathepsin B. The reactions were run at 37 °C for either 4 min (plasmin) or 20 min (cathepsin B) and were then quenched and precipitated with 60 μL of absolute ethanol and stored at −20 °C for a minimum of 2 h. The samples were centrifuged for 5 min at 15000*g*, and the supernatants were analyzed by RP-HPLC as above. Rates of reaction, in μM/min, were calculated and fit with nonlinear least-squares analysis. Each reaction was performed in triplicate.

Human Plasma Stability. To assay for the stability of the prodrug in blood plasma, **2b** was diluted with human plasma collected from healthy individuals (a gift from Somalogic, Inc., Boulder, CO) to a final drug concentration of 50 μM. The reaction was incubated at 37 °C for 24 h. Aliquots were taken at 0.25, 1, 3, 8, 12, and 24 h, quenched with an equal volume of ethanol, and incubated at −20 °C overnight to precipitate the proteins. Precipitated protein was removed by centrifugation in a desktop centrifuge for 5 min at 15000*g*. The supernatant was analyzed by RP-HPLC (plasma method: acetonitrile from 20% to 40% over 5 min, to 70% at 10 min, to 80% at 13 min, isocratic for 2 min, then back to 20% by 17 min). The percent compositions of **2b** (eluting at 8−9 min) and dox (eluting at 6.5−7.0 min) were determined from their relative absorbances at 480 nm, taking into account all other unknown products that appeared during the reaction and absorbed at 480 nm. The experiment was repeated in triplicate.

IC_{50} Assays. Initial characterization of **2b** was performed in MiaPaCa-2 human pancreatic carcinoma and MCF-7 human breast cancer cell lines. The cells were seeded into 96-well plates at a density of 1000 cells/well and allowed to adhere overnight. The medium was replaced with 90 μL of serum-free medium containing one or more of plasmin (0.2 U/well), trypsin (0.2 U/well), cathepsin B (0.2 U/well), aprotinin (5 μM, Research Products International, Mt. Prospect, IL), or Complete Mini protease inhibitors (1× according to package instructions, Roche Applied Science, Indianapolis, IN). **2b** (10 μL) was added to the wells for final concentrations between 2000 and 1 nM, and controls received only vehicle (either DMSO or saline with 10% PEG). The cells were treated with **2b** and activator/inhibitor for 24 h, at which point the treatment medium was replaced with Complete medium and the cells were allowed to grow for 5 days or until the control wells reached 80% confluency, whichever was shorter. The cells were then fixed with 5% formalin in PBS for 10 min and stained with crystal violet (0.01% w/v in water) for 20−30 min. The plates were rinsed and air-dried, and the stain was redissolved either in a mixture of ethanol, water, and methanol (6:3:1) or in 2-propanol/water (1:1) with 2% sodium dodecylsulfate (SDS). Cell density was measured by absorbance at 582 nm. Percent optical density, relative to control wells, was fit to a variable slope sigmoidal dose−response curve by nonlinear regression analysis in GraphPad Prism 5.0. These experiments indicated that pure DMSO formulations or saline/PEG/phosphate formulations of **2b** resulted in identical growth inhibition.

Following initial tests in MiaPaCa-2 and MCF-7 cells, tests with **2b** alone or with plasmin (0.2 U/well) were performed on an array of pancreatic cancer lines (BxPC3, L3.3, L3.5, and L3.6PL), a small-cell lung cancer line (SHP77), and an ovarian cancer line (NCI-RES/Adr), as well as a nontumor derived cell line (HEK-293T). All experiments were performed identically as described above.

Cellular Uptake. MCF-7 or MiaPaCa-2 cells were plated into six-well plates at a density of 250 000 cells/well and allowed to adhere overnight. The medium was then replaced with serum free medium, and 0.5 μM **2b** or 0.5 μM **2b** + 0.2 U plasmin was added (final concentrations). The cells were incubated for up to 5 h, then trypsinized and analyzed for the presence of the anthracycline fluorophore by flow cytometry (FL3 channel). The mean fluorescence values were converted to fold-over background, in which background was defined as cells receiving no **2b**.

■ ASSOCIATED CONTENT

Ⓢ Supporting Information

Synthetic methods for **1b** and NMR spectra for **10** and **2b**. This material is available free of charge via the Internet at http://pubs.acs.org.

■ AUTHOR INFORMATION

Corresponding Author

*Phone: 303-492-6193. Fax: 303-492-5849. E-mail: tad.koch@colorado.edu.

Present Address

†GSK Biologics, 553 Old Corvalis Road, Hamilton, MT 59840.

Notes

The authors declare no competing financial interest.

■ ACKNOWLEDGMENTS

The authors acknowledge Wells Messersmith and John Arcaroli at the University of Colorado, Anschutz Medical Campus, for the pancreatic cell lines L3.3, L3.5, and L3.6PL. Somalogic, Inc. of Boulder, CO, provided the gift of the human plasma. We thank Rich Shoemaker for help with NMR protocols; Glen Post, Jordan Nafie, and Nick Taylor for synthetic work; and Kristen Barthel for careful reading of the manuscript. We are thankful for Bioscience Discovery Evaluation Grants 07-00018 and 11BGF-34 from the State of Colorado and the University of Colorado Office of Technology Transfer and NIH Grants R41 CA12424, R21 CA143549, and R21 CA141101 for funding this research.

ABBREVIATIONS USED

aFK, D-Ala-L-Phe-L-Lys; aFK-Dox, *N*-(*N*-(D-alanyl-L-phenylalanyl-L-lysyl)-*p*-aminobenzyloxycarbonyl)doxorubicin; aFK-Doxaz, *N*-(*N*-(D-alanyl-L-phenylalanyl-L-lysyl)-*p*-aminobenzyloxycarbonyl)doxazolidine; alloc, allyloxycarbonyl; CES2/hiCE, carboxylesterase 2; dox, doxorubicin; doxaz, doxazolidine; doxf, doxoform; ECM, extracellular matrix; Fmoc, 9-fluorenylmethyloxycarbonyl; Fmoc-OSu, *N*-Fmoc-*N*-hydroxysuccinimide; GaFK-Doxaz, *N*-(*N*-(*N*-acetylglycyl-D-alanyl-L-phenylalanyl-L-lysyl)-*p*-aminobenzyloxycarbonyl)-doxazolidine; HBTU, 2-(1*H*-benzotriazole-1-yl)-1,1,3,3-tetramethyluronium hexafluorophosphate; HOBt, 1-hydroxybenzotriazole; IC_{50}, inhibitory concentration 50%; MDR, multidrug resistant; MMP, matrix metalloprotease; NAC, *N*-acetylcysteine; P170GP, P-170 glycoprotein; PABA, *p*-aminobenzyl alcohol; PABC, *p*-aminobenzyloxycarbonyl; PBS, phosphate buffered saline; PEG, polyethylene glycol; pNP, *p*-nitrophenyl; PPD, pentyl PABC-Doxaz; RP-HPLC, reverse phase high performance liquid chromatography; SPPS, solid-phase peptide synthesis; TFA, trifluoroacetic acid; tPA, tissue plasminogen activator; U, unit; uPA, urokinase plasminogen activator

REFERENCES

(1) Saltiel, E.; McGuire, W. Doxorubicin (adriamycin) cardiomyopathy. *West. J. Med.* **1983**, *139*, 332−341.

(2) Takemura, G.; Fujiwara, H. Doxorubicin-induced cardiomyopathy from the cardiotoxic mechanisms to management. *Prog. Cardiovasc. Dis.* **2007**, *49*, 330−352.

(3) Nielsen, D.; Maare, C.; Skovsgaard, T. Cellular resistance to anthracyclines. *Gen. Pharmacol.* **1996**, *27*, 251−255.

(4) Myers, C. E.; McGuire, W. P.; Liss, R. H.; Ifrim, I.; Grotzinger, K.; Young, R. C. Adriamycin: the role of lipid peroxidation in cardiac toxicity and tumor response. *Science* **1977**, *197*, 165−167.

(5) Siveski-Iliskovic, N.; Hill, M.; Chow, D. A.; Singal, P. K. Probucol protects against adriamycin cardiomyopathy without interfering with its antitumor effect. *Circulation* **1995**, *91*, 10−15.

(6) Weiss, R. B. The anthracyclines: Will we ever find a better doxorubicin? *Semin. Oncol.* **1992**, *19*, 670−686.

(7) Krown, S. E.; Northfelt, D. W.; Osoba, D.; Stewart, J. S. Use of liposomal anthracyclines in Kaposi's sarcoma. *Semin. Oncol.* **2004**, *31*, 36−52.

(8) Robert, N. J.; Vogel, C. L.; Henderson, I. C.; Sparano, J. A.; Moore, M. R.; Silverman, P.; Overmoyer, B. A.; Shapiro, C. L.; Park, J. W.; Colbern, G. T.; Winer, E. P.; Gabizon, A. A. The role of the liposomal anthracyclines and other systemic therapies in the management of advanced breast cancer. *Semin. Oncol.* **2004**, *31*, 106−146.

(9) Lorusso, D.; Di Stefano, A.; Carone, V.; Fagotti, A.; Pisconti, S.; Scambia, G. Pegylated liposomal doxorubicin-related palmar-plantar erythrodysesthesia ("hand−foot" syndrome). *Ann. Oncol.* **2007**, *18*, 1159−1164.

(10) Post, G. C.; Barthel, B. L.; Burkhart, D. J.; Hagadorn, J. R.; Koch, T. H. Doxazolidine, a proposed active metabolite of doxorubicin that cross-links DNA. *J. Med. Chem.* **2005**, *48*, 7648−7657.

(11) Kalet, B. T.; McBryde, M. B.; Espinosa, J. M.; Koch, T. H. Doxazolidine induction of apoptosis by a topoisomerase II independent mechanism. *J. Med. Chem.* **2007**, *50*, 4493−4500.

(12) Fenick, D. J.; Taatjes, D. J.; Koch, T. H. Doxoform and daunoform: anthracycline−formaldehyde conjugates toxic to resistant tumor cells. *J. Med. Chem.* **1997**, *40*, 2452−2461.

(13) Burkhart, D. J.; Barthel, B. L.; Post, G. C.; Kalet, B. T.; Nafie, J. W.; Shoemaker, R. K.; Koch, T. H. Design, synthesis, and preliminary evaluation of doxazolidine carbamates as prodrugs activated by carboxylesterases. *J. Med. Chem.* **2006**, *49*, 7002−7012.

(14) Barthel, B. L.; Torres, R. C.; Hyatt, J. L.; Edwards, C. C.; Hatfield, M. J.; Potter, P. M.; Koch, T. H. Identification of human intestinal carboxylesterase as the primary enzyme for activation of a doxazolidine carbamate prodrug. *J. Med. Chem.* **2008**, *51*, 298−304.

(15) Barthel, B. L.; Zhang, Z.; Rudnicki, D. L.; Coldren, C. D.; Polinkovsky, M.; Sun, H.; Koch, G. G.; Chan, D. C.; Koch, T. H. Preclinical efficacy of a carboxylesterase 2-activated prodrug of doxazolidine. *J. Med. Chem.* **2009**, *52*, 7678−7688.

(16) Cecchin, E.; Corona, G.; Masier, S.; Biason, P.; Cattarossi, G.; Frustaci, S.; Buonadonna, A.; Colussi, A.; Toffoli, G. Carboxylesterase isoform 2 mRNA expression in peripheral blood mononuclear cells is a predictive marker of the irinotecan to SN38 activation step in colorectal cancer patients. *Clin. Cancer Res.* **2005**, *11*, 6901−6907.

(17) Duffy, M. J.; O'Grady, P.; Devaney, D.; O'Siorain, L.; Fennelly, J. J.; Lijnen, H. R. Tissue-type plasminogen activator, a new prognostic marker in breast cancer. *Cancer Res.* **1988**, *48*, 1348−1349.

(18) Giannelli, G.; Falk-Marzillier, J.; Schiraldi, O.; Stetler-Stevenson, W. G.; Quaranta, V. Induction of cell migration by matrix metalloprotease-2 cleavage of laminin-5. *Science* **1997**, *277*, 225−228.

(19) Bemis, L. T.; Schedin, P. Reproductive state of rat mammary gland stroma modulates human breast cancer cell migration and invasion. *Cancer Res.* **2000**, *60*, 3414−3418.

(20) Choong, P. F.; Nadesapillai, A. P. Urokinase plasminogen activator system: a multifunctional role in tumor progression and metastasis. *Clin. Orthop. Relat. Res.* **2003**, S46−58.

(21) Lijnen, H. R. Plasmin and matrix metalloproteinases in vascular remodeling. *Thromb. Haemostasis* **2001**, *86*, 324−333.

(22) Ulisse, S.; Baldini, E.; Sorrenti, S.; D'Armiento, M. The urokinase plasminogen activator system: a target for anti-cancer therapy. *Curr. Cancer Drug Targets* **2009**, *9*, 32−71.

(23) Cobos, E.; Jumper, C.; Lox, C. Pretreatment determination of the serum urokinase plasminogen activator and its soluble receptor in advanced small-cell lung cancer or non-small-cell lung cancer. *Clin. Appl. Thromb./Hemostasis* **2003**, *9*, 241−246.

(24) Werle, B.; Kotzsch, M.; Lah, T. T.; Kos, J.; Gabrijelcic-Geiger, D.; Spiess, E.; Schirren, J.; Ebert, W.; Fiehn, W.; Luther, T.; Magdolen, V.; Schmitt, M.; Harbeck, N. Cathepsin B, plasminogenactivator-inhibitor (PAI-1) and plasminogenactivator-receptor (uPAR) are prognostic factors for patients with non-small cell lung cancer. *Anticancer Res.* **2004**, *24*, 4147−4161.

(25) D'Amico, T. A.; Brooks, K. R.; Joshi, M. B.; Conlon, D.; Herndon, J.; Petersen, R. P.; Harpole, D. H. Serum protein expression predicts recurrence in patients with early-stage lung cancer after resection. *Ann. Thorac. Surg.* **2006**, *81*, 1982−1987 ; discussion 1987.

(26) De Petro, G.; Tavian, D.; Copeta, A.; Portolani, N.; Giulini, S. M.; Barlati, S. Expression of urokinase-type plasminogen activator (u-PA), u-PA receptor, and tissue-type PA messenger RNAs in human hepatocellular carcinoma. *Cancer Res.* **1998**, *58*, 2234−2239.

(27) Zheng, Q.; Tang, Z. Y.; Xue, Q.; Shi, D. R.; Song, H. Y.; Tang, H. B. Invasion and metastasis of hepatocellular carcinoma in relation to urokinase-type plasminogen activator, its receptor and inhibitor. *J. Cancer Res. Clin. Oncol.* **2000**, *126*, 641−646.

(28) Takeuchi, Y.; Nakao, A.; Harada, A.; Nonami, T.; Fukatsu, T.; Takagi, H. Expression of plasminogen activators and their inhibitors in human pancreatic carcinoma: immunohistochemical study. *Am. J. Gastroenterol.* **1993**, *88*, 1928−1933.

(29) Cantero, D.; Friess, H.; Deflorin, J.; Zimmermann, A.; Brundler, M. A.; Riesle, E.; Korc, M.; Buchler, M. W. Enhanced expression of urokinase plasminogen activator and its receptor in pancreatic carcinoma. *Br. J. Cancer* **1997**, *75*, 388−395.

(30) Shin, S. J.; Kim, K. O.; Kim, M. K.; Lee, K. H.; Hyun, M. S.; Kim, K. J.; Choi, J. H.; Song, H. S. Expression of E-cadherin and uPA and their association with the prognosis of pancreatic cancer. *Jpn. J. Clin. Oncol.* **2005**, *35*, 342−348.

(31) de Groot, F. M. H.; de Bart, A. C. W.; Verheijen, J. H.; Scheeren, H. W. Synthesis and biological evaluation of novel prodrugs of anthracyclines for selective activation by the tumor-associated protease plasmin. *J. Med. Chem.* **1999**, *42*, 5277−5283.

(32) Devy, L.; de Groot, F. H. M.; Blacher, S.; Hajitou, A.; Beusker, P.; Scheeren, W.; Foldart, J.-M.; Noel, A. Plasmin-activated doxorubicin

prodrugs containing a spacer reduce tumor growth and angiogenesis without systemic toxicity. *FASEB J.* **2004**, *18*, 565−567.
(33) Carl, P. L.; Chakravarty, P. K.; Katzenellenbogen, J. A. A novel connector linkage applicable in prodrug design. *J. Med. Chem.* **1981**, *24*, 479−480.
(34) Low, T. L.; Goldstein, A. L. The chemistry and biology of thymosin. II. Amino acid sequence analysis of thymosin alpha1 and polypeptide beta1. *J. Biol. Chem.* **1979**, *254*, 987−995.
(35) Abiko, T.; Sekino, H. Synthesis of an immunologically active fragment analog of prothymosin alpha with enhanced enzymatic stability. *Chem. Pharm. Bull. (Tokyo)* **1991**, *39*, 752−756.
(36) Nguyen, L. T.; Chau, J. K.; Perry, N. A.; de Boer, L.; Zaat, S. A.; Vogel, H. J. Serum stabilities of short tryptophan- and arginine-rich antimicrobial peptide analogs. *PLoS One* **2010**, 5.
(37) Kos, J.; Werle, B.; Lah, T.; Brunner, N. Cysteine proteinases and their inhibitors in extracellular fluids: markers for diagnosis and prognosis in cancer. *Int. J. Biol. Markers* **2000**, *15*, 84−89.
(38) Jedeszko, C.; Sloane, B. F. Cysteine cathepsins in human cancer. *Biol. Chem.* **2004**, *385*, 1017−1027.
(39) Joyce, J. A.; Baruch, A.; Chehade, K.; Meyer-Morse, N.; Giraudo, E.; Tsai, F. Y.; Greenbaum, D. C.; Hager, J. H.; Bogyo, M.; Hanahan, D. Cathepsin cysteine proteases are effectors of invasive growth and angiogenesis during multistage tumorigenesis. *Cancer Cell* **2004**, *5*, 443−453.
(40) Dubowchik, G. M.; Firestone, R. A.; Padilla, L.; Willner, D.; Hofstead, S. J.; Mosure, K.; Knipe, J. O.; Lasch, S. J.; Trail, P. A. Cathepsin B-labile dipeptide linkers for lysosomal release of doxorubicin from internalizing immunoconjugates: model studies of enzymatic drug release and antigen-specific in vitro anticancer activity. *Bioconjugate Chem.* **2002**, *13*, 855−869.
(41) Schmid, B.; Chung, D. E.; Warnecke, A.; Fichtner, I.; Kratz, F. Albumin-binding prodrugs of camptothecin and doxorubicin with an Ala-Leu-Ala-Leu-linker that are cleaved by cathepsin B: synthesis and antitumor efficacy. *Bioconjugate Chem.* **2007**, *18*, 702−716.
(42) Misaka, E.; Tappel, A. L. Inhibition studies of cathepsins A, B, C and D from rat liver lysosomes. *Comp. Biochem. Physiol., Part B* **1971**, *38*, 651−662.
(43) Hirao, T.; Hara, K.; Takahashi, K. Purification and characterization of cathepsin B from monkey skeletal muscle. *J. Biochem.* **1984**, *95*, 871−879.
(44) Agarwal, S. K.; Choudhury, S. D.; Lamsal, M.; Khan, M. Y. Catalytic and physico-chemical characteristics of goat spleen cathepsin B. *Biochem. Mol. Biol. Int.* **1997**, *42*, 1215−1226.
(45) Lechuga, C. G.; Hernandez-Nazara, Z. H.; Hernandez, E.; Bustamante, M.; Desierto, G.; Cotty, A.; Dharker, N.; Choe, M.; Rojkind, M. PI3K is involved in PDGF-beta receptor upregulation post-PDGF-BB treatment in mouse HSC. *Am. J. Physiol.: Gastrointest. Liver Physiol.* **2006**, *291*, G1051−1061.
(46) Fehske, K. J.; Muller, W. E.; Wollert, U. The location of drug binding sites in human serum albumin. *Biochem. Pharmacol.* **1981**, *30*, 687−692.
(47) Kratochwil, N. A.; Huber, W.; Muller, F.; Kansy, M.; Gerber, P. R. Predicting plasma protein binding of drugs: a new approach. *Biochem. Pharmacol.* **2002**, *64*, 1355−1374.
(48) Koivunen, E.; Ristimaki, A.; Itkonen, O.; Osman, S.; Vuento, M.; Stenman, U. H. Tumor-associated trypsin participates in cancer cell-mediated degradation of extracellular matrix. *Cancer Res.* **1991**, *51*, 2107−2112.
(49) Miszczuk-Jamska, B.; Merten, M.; Guy-Crotte, O.; Amouric, M.; Clemente, F.; Schoumacher, R. A.; Figarella, C. Characterization of trypsinogens 1 and 2 in two human pancreatic adenocarcinoma cell lines; CFPAC-1 and CAPAN-1. *FEBS Lett.* **1991**, *294*, 175−178.
(50) Yamamoto, H.; Iku, S.; Itoh, F.; Tang, X.; Hosokawa, M.; Imai, K. Association of trypsin expression with recurrence and poor prognosis in human esophageal squamous cell carcinoma. *Cancer* **2001**, *91*, 1324−1331.
(51) Santin, A. D.; Cane, S.; Bellone, S.; Bignotti, E.; Palmieri, M.; De Las Casas, L. E.; Anfossi, S.; Roman, J. J.; O'Brien, T.; Pecorelli, S. The novel serine protease tumor-associated differentially expressed gene-15 (matriptase/MT-SP1) is highly overexpressed in cervical carcinoma. *Cancer* **2003**, *98*, 1898−1904.
(52) Nolan, C.; Hall, L. S.; Barlow, G. H.; Tribby, I. I. E. Plasminogen activator from human embryonic kidney cell cultures. Evidence for a proactivator. *Biochim. Biophys. Acta* **1977**, *496*, 384−400.
(53) Carl, P. L.; Chakravarty, P. K.; Katzenellenbogen, J. A.; Weber, M. J. Protease-activated "prodrugs" for cancer chemotherapy. *Proc. Natl. Acad. Sci. U.S.A.* **1980**, *77*, 2224−2228.
(54) Gude, M.; Ryf, J.; White, P. An accurate method for quantitation of Fmoc-derivitized solid phase supports. *Lett. Pept. Sci.* **2002**, *9*, 203−206.